Technical Innovations & Patient Support in Radiation Oncology 34 (2025) 100305

Contents lists available at ScienceDirect

Technical Innovations & Patient Support in Radiation Oncology

journal homepage: www.sciencedirect.com/journal/technical-innovations-and-patient-support-in-radiation-oncology

Research Article

Evaluation of MRI anatomy in machine learning predictive models to assess hydrogel spacer benefit for prostate cancer patients

Madison Bush [a], Scott Jones [a,b], Catriona Hargrave [a,b,*]

[a] Queensland University of Technology, Faculty of Health, School of Clinical Sciences, Brisbane, Queensland, Australia
[b] Radiation Oncology Princess Alexandra Hospital Raymond Terrace (ROPART), South Brisbane, Queensland, Australia

ARTICLE INFO

Keywords:
Radiation Therapy
Machine Learning
Toxicity Prediction
Dose Prediction
Hydrogel Spacer

ABSTRACT

Introduction: Hydrogel spacers (HS) are designed to minimise the radiation doses to the rectum in prostate cancer radiation therapy (RT) by creating a physical gap between the rectum and the target treatment volume inclusive of the prostate and seminal vesicles (SV). This study aims to determine the feasibility of incorporating diagnostic MRI (dMRI) information in statistical machine learning (SML) models developed with planning CT (pCT) anatomy for dose and rectal toxicity prediction. The SML models aim to support HS insertion decision-making prior to RT planning procedures.

Methods: Regions of interest (ROIs) were retrospectively contoured on the pCT and registered dMRI scans for 20 patients. ROI Dice and Hausdorff distance (HD) comparison metrics were calculated. The ROI and patient clinical risk factors (CRFs) variables were inputted into three SML models and then pCT and dMRI-based dose and toxicity model performance compared through confusion matrices, AUC curves, accuracy performance metric results and observed patient outcomes.

Results: Average Dice values comparing dMRI and pCT ROIs were 0.81, 0.47 and 0.71 for the prostate, SV, and rectum respectively. Average Hausdorff distances were 2.15, 2.75 and 2.75 mm for the prostate, SV, and rectum respectively. The average accuracy metric across all models was 0.83 when using dMRI ROIs and 0.85 when using pCT ROIs.

Conclusion: Differences between pCT and dMRI anatomical ROI variables did not impact SML model performance in this study, demonstrating the feasibility of using dMRI images. Due to the limited sample size further training of the predictive models including dMRI anatomy is recommended.

Introduction

Radiation therapy (RT) is widely used in the treatment of prostate cancer to improve local tumour control [1]. Despite the development of highly conformal treatment techniques and image guided radiotherapy, the rectum is still a dose-limiting structure due to its proximity to the prostate [1–3]. In addition to the received radiation dose, clinical risk factors (CRFs) such as diabetes, previous abdominal surgery, haemorrhoids, or use of anticoagulant drugs have been associated with post-RT rectal toxicities [4].

Hydrogel spacers (HS) are designed to create a physical gap between the rectum and prostate [5], thus minimising radiation dose to the rectum. HS are either a saline inflated balloon or a liquid gel that solidifies [5,6]. Some non-randomised controlled trials provide predicted values of HS decreasing rectal complications in 20 % of patients [7], and others estimate that a HS reduces grade 2+ toxicity from 10.1 % to 3.8 % [8]. However, some men have a natural space between the rectum and prostate and may not gain any dosimetric benefit from the invasive and costly procedure [4,9,10]. Caine et al have previously shown that an individual's anatomy can influence dosimetric protocol compliance for prostate radiation therapy [11]. Fischer-Valuck et al developed a symmetry score utilising MRI simulation to evaluate HS distribution and

Abbreviations: CART, Classification and Regression Tree Model; CRFs, Clinical Risk Factors; DICOM, Digital Imaging and Communications in Medicine; dMRI, Diagnostic Magnetic Resonance Imaging; HD, Hausdorff Distance; HS, Hydrogel Spacer; LR, Logistic Regression Model; MRI, Magnetic Resonance Imaging; OAR, Organ at Risk; pCT, Planning Computed Tomography; PTV, Planning Target Volume; RF, Random Forest Model; ROI, Region of Interest; ROPART, Radiation Oncology Princess Alexandra Raymond Terrace; RT, Radiation Therapy; SML, Statistical Machine Learning; SV, Seminal Vesicles.

* Corresponding author at: Catriona Hargrave, Queensland University of Technology, 2 George Street, Brisbane, QLD, 4000, Australia.
E-mail address: c.hargrave@qut.edu.au (C. Hargrave).

https://doi.org/10.1016/j.tipsro.2025.100305
Received 14 October 2024; Received in revised form 13 January 2025; Accepted 7 February 2025
Available online 26 February 2025

rectal dose reduction due to the clarity of the biomaterial of the HS on diagnostic magnetic resonance imaging (dMRI) scans [12]. Grossman et al also developed a quality metric for HS insertion based on prostate-rectal interspace to be more relevant to rectal dosimetry in treatment planning [13]. To assist in HS decision making, investigations into HS benefit based on individual patient anatomy and CRFs have been conducted using predictive modelling [4,9,10].

While there are studies that use planning CT (pCT) data with a calculated plan or planning target volume (PTV) to assess the need for HS or use dMRI scans for assessing HS placement, to date, there are no current studies addressing rectal toxicity and dose prediction solely from the dMRI data. Studies that use predictive modelling on pCT data occur too late in the clinical process. If HS is indicated for the patient, the treatment planning process including the pCT needs to be repeated after HS insertion. Jones et al's [9] study has a unique approach of a model incorporating anatomical regions of interest (ROIs) from the pCT and patient CRFs to predict rectal toxicity. These models introduce the possibility of applying their predictive models to diagnostic images obtained prior to any RT procedures [9]. Use of dMRI scans acquired prior to pCT to determine anatomical ROIs as predictive model input variables could minimise resources such as repeat pCT imaging after HS insertions as well as time expenditure in the current HS decision-making process. Uncertainties involving the use of MRI in RT include registration accuracy with the pCT, contouring variability and anatomical spatial relationship due to reduced interobserver variability and volume size disagreements attributable to variations in bladder and bowel preparation [7,14]. As a result, this study aimed to investigate the feasibility of incorporating dMRI data in dose and toxicity statistical machine learning (SML) models previously developed by Jones et al [9,10] and evaluated the similarity of the pCT and dMRI-based ROIs and the model outputs.

Methods

Patient data for dMRI-based model evaluation

Institutional ethics approval was granted for the current study. Jones et al's [9,10] previous study involved 176 prostate cancer patients with the inclusion criteria of males over the age of 18, radical treatment intent, complete and standard fractionation external beam radiation therapy treatment to a prescription dose of 74–78 Gy in 37–39 fractions, intact prostate +/- nodal involvement, intensity modulated radiation therapy (IMRT) or volumetric modulated arc therapy (VMAT) dose techniques and registered dMRI scans. The 20 most recently treated of these patients were retrospectively selected for the current study.

Description of model variables and development

The ROIs used in the development of Jones et al's [9] SML models are described in Table 1. The three SML models that were investigated to predict toxicity and dose outcomes were random forest (RF), logistic regression (LR) and classification and regression tree (CART), which are common methods for binary classification [15]. The ROIs, dosimetric profiles (See Table 2) and the recorded patient rectal toxicity data (using colonoscopy status as a Grade 2 toxicity surrogate), were used to develop the predictive models for Jones et al's [9] study.

Generation of dMRI ROIs

Patient treatment plans and their pCT were restored from the Pinnacle Version 16.2 (Philips Healthcare, Fitchburg, WI) treatment planning system archive. The T2 weighted dMRI scans were either already registered with a patient's plan or imported from the picture archiving and communication system and registered with the restored plan. To ensure consistency regardless of bowel and bladder variations, the prostate and rectal wall interface were prioritised in the scan fusions, as per standard image matching protocols in the department where data was acquired [16].

The prostate, SV, and rectum on the dMRI scans were contoured and scripts were used to replicate the generation of the overlap and high dose rectal ROIs (Table 1). The dMRI contours were created by the same investigator and checked by at least one other investigator. The SV ROIs were typically contoured 1 cm proximal to the prostate, as per the clinical protocol at the time for the department where data was obtained. The dMRI SV number of slices contoured were selected to match pCT SV contour length. As the dMRI scans were generally shorter in length than the pCT, the dMRI rectum was extrapolated past the dMRI scan to match the contoured pCT length. All contours were cleaned using the ROI clean tool in Pinnacle V16.2 to remove small islands less than 0.1 cc, produced from the Boolean operations for contour development, before scripts were run to create predictor ROIs.

Table 1
Description of ROI variables developed by Jones et al. [9].

Description	Abbreviation	Source
Prostate	PROS_VOL	Prostate
Proximal Seminal Vesicle	SV_VOL	Proximal Seminal Vesicle
Rectum	REC_SOL_VOL	Solid Rectum
High Dose Rectum truncated to prostate limits	HD_REC_VOL	Solid Rectum truncated at superior & inferior limits of Prostate
High Dose Rectum as a percentage of the whole rectum truncated to prostate limits	HD_REC_PERC	Solid Rectum truncated at superior & inferior limits of Prostate, as a percentage of the whole Solid Rectum
High Dose Rectum truncated to prostate and Proximal Seminal Vesicle limits	HD_REC_VOL_SV	Solid Rectum truncated at superior limit of Proximal Seminal Vesicle & inferior limit of Prostate
High Dose Rectum as a percentage of the whole Rectum truncated to Prostate and Proximal Seminal Vesicle limits	HD_SV_REC_PERC	Solid Rectum truncated at superior limit of Proximal Seminal Vesicle & inferior limit of Prostate, as a percentage of whole Solid Rectum
Overlap between Prostate expanded 5 mm in all directions and Solid Rectum	PROS_EXP_RECT	The overlap between Prostate expanded 5 mm in all directions and the Solid Rectum
Overlap between Prostate expanded 5 mm in all directions and Rectum as a percentage of the Solid Rectum	PROS_EXP_PERC	The overlap between Prostate expanded 5 mm in all directions and the Solid Rectum, as a percentage of the Solid Rectum
Overlap between combined Prostate and Proximal Seminal Vesicles expanded 5 mm in all directions and Solid Rectum	PSV_EXP_RECT	The overlap between Prostate and Proximal Seminal Vesicle expanded 5 mm in all directions and the Solid Rectum
Overlap between Prostate and Proximal Seminal Vesicle expanded 5 mm in all directions and Rectum as a percentage of the Solid Rectum	PSV_EXP_PERC	The overlap between Prostate & Proximal Seminal Vesicle expanded 5 mm in all directions and the Solid Rectum, as a percentage of the Solid Rectum

Table 2
Relative rectal dose levels and classification categories used by Jones et al. [9].

Dose Level	Volume Threshold Tolerance Achieved (classification = Y)	Volume Threshold Breach (classification = N)
V50	<35 % volume	>35 % volume
V83	<17 % volume	>17 % volume
V96	<7 % volume	>7 % volume

dMRI and pCT ROI comparison

The dMRI and pCT scans as well as their associated ROIs were exported from Pinnacle as Digital Imaging and Communications in Medicine (DICOM) RT files and imported into 3D slicer (https://slicer.org/). To compare volume differences between the dMRI and pCT anatomy, the volume, Dice and Hausdorff distance (HD) metrics were calculated for each ROI [17,18]. The ROI data was tested for normal distribution, and then either a paired *t*-test or Wilcoxen signed rank test was used to compare the means of dMRI and pCT ROIs with $p < 0.05$ considered statistically significant. The extrapolation of the rectum dMRI ROIs was not considered in the statistical testing or comparison of volume differences and may influence the accuracy of these results.

Model performance with dMRI data

The dMRI and pCT ROI volume information for the 20 patients as well as the CRFs, treatment plan rectal dose levels and toxicity outcomes collected in Jones et al's [9,10] study were collated. The rectal dose levels included the volume receiving 50 %, 83 % and 96 % (V50, V83 and V96 respectively). The CRFs included for the modelling comprised of whether the patient had surgery, classified into yes (A) or no (B), diabetes which was divided as yes – type 2 (A), yes – type 1 (B) or no (C), and the use of anticoagulants was answered as yes (A), low dose aspirin (B) or no (C). The toxicity outcome surrogate used in the SML models was whether the patient had a symptom-induced colonoscopy (equivalent to grade 2 toxicity of rectal bleeding [19]) and was grouped as yes (Y) or no (N). First, the pCT ROI data and CRF data was inputted into the previously created predictive models using R statistical software. Then, the dMRI ROIs and CRFs were used as variable inputs in the models.

A confusion matrix used to calculate accuracy, sensitivity, specificity, negative predictive value, and positive predictive values was generated to analyse model performance. The accuracy performance metric compares the Y or N class prediction of whether a colonoscopy was performed between the SML prediction and actual patient outcomes. Sensitivity and specificity depend on a single cut point used to classify a test result as positive [20]. The model performance metric of the area under the receiver operator characteristic curve (AUC) was also calculated and plotted. The perfect model prediction is denoted by a result of 1, however, the value associated with clinical significance within the literature and deemed as performing better than random chance was selected as >0.7 for the study [20].

Results

dMRI and pCT ROI comparison

For the total 20 patients included in this feasibility study, the mean prostate, seminal vesicle, and solid rectum volumes for the dMRI ROIs were 35.6 cm^3, 7.91 cm^3 and 51.27 cm^3 respectively and the pCT ROIs were 36.65 cm^3, 8.14 cm^3 and 57.32 cm3, respectively. The ROI volumes for the two imaging modalities were similar (Fig. 1). The greatest discrepancy of volumes was observed in the rectal volumes. For a single patient, there was a difference in contour size of 61.69 cm^3 which was an increase of 47.79 % from their dMRI to pCT. However, overall, only a small 10.55 % difference was observed for the average across all patients. The high dose rectum variables and expanded overlap variables (Fig. 1) also did not show considerable differences between dMRI and pCT scans.

An average Dice of 0.81 was recorded for all prostate dMRI and pCT ROI comparisons. The rectum ROI generated an average Dice of 0.71, whilst the seminal vesicles produced an average Dice value of 0.47 (Fig. 2). The PROS_EXP_RECT generated an average Dice of 0.33 which indicates a low degree of similarity for these contours. The range of the average and maximum HD results are depicted in Fig. 2. The greatest difference in average HD values was observed for the PSV_EXP_RECT with 3.58 mm. In the calculation of the maximum HD results, the PSV_EXP_RECT produced a result of 16.00 mm as the greatest discrepancy between dMRI and pCT scans.

In all ROI mean comparisons, only the HD_REC_PERC and HD_SV_REC_PERC ROIs produced statistically significant results ($p < 0.05$) between dMRI and pCT of $p = 0.001$ and $p = 0.009$ respectively (Supporting Information).

Although the SV dMRI and pCT means and statistical significance testing did not indicate large differences in their volume, it was observed during data collection that the location of this organ could change drastically between the two imaging modalities (Fig. 3).

Model performance with dMRI data

The AUC curves for all rectal toxicity and dose level SML models are depicted in Fig. 4 for both dMRI and pCT scans. In Table 3, the model performance metrics are demonstrated across all SML prediction models. On average, the accuracy for dMRI toxicity predictions was 0.83 across all three SML models and the pCT average was a comparable 0.85. The dMRI results for the three dose levels of V50, V83 and V96 were averaged as 0.65, 0.27 and 0.38 respectively with pCT values of 0.78, 0.33 and 0.40. The average for dMRI toxicity AUC outcome produced a result of 0.59, with the pCT generating a result of 0.65. The AUC for the rectal levels of V50, V83 and V96 for dMRI were 0.55, 0.62 and 0.52 with pCT results of 0.70, 0.61 and 0.55, respectively. There were no large discrepancies observed between the sensitivity, specificity, positive predictive value, and negative predictive values and the individual predictions were similar between imaging modalities (Supporting Information). In comparison of the specific models, RF performed best for the toxicity predictions for both dMRI and pCT. The CART SML model generated the most accurate results for the V50 dose level and LR SML model for the V96 dose level for both imaging modalities. For the V83 dose level, CART produced the best results for dMRI and RF performed

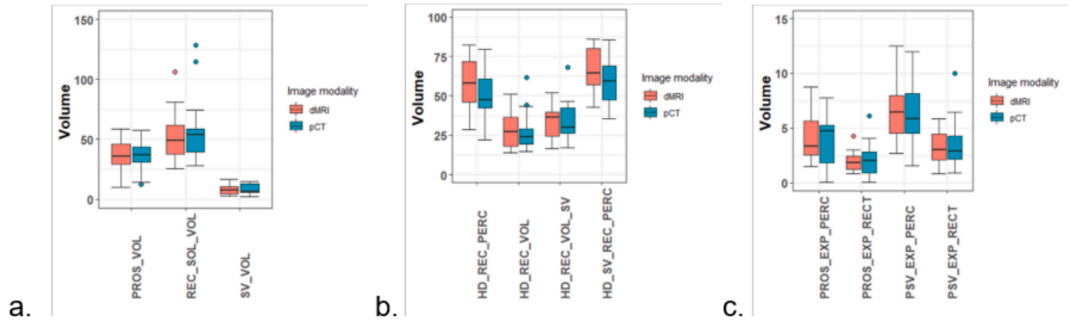

Fig. 1. Boxplots of all dMRI and pCT ROI volumes. *A. Prostate, rectum and seminal vesicle volumes (cm^3), B. High dose rectal ROIs (cm^3 for those ending in VOL and % of total volume for those ending in PERC) and c. overlap volumes (% of total volume for those ending in PERC, and cm^2 for the others).*

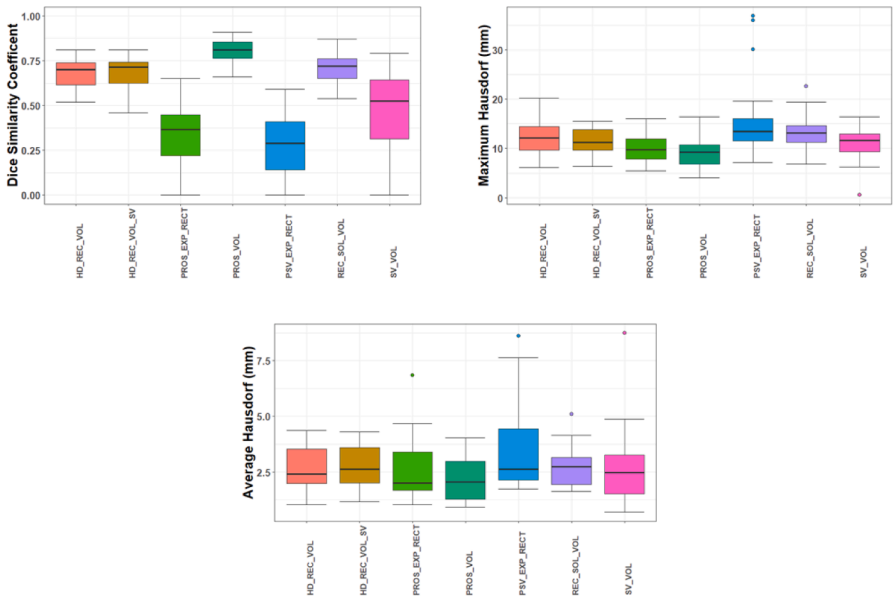

A. Dice boxplots, B. Maximum HD (mm) boxplots, C. Average HD (mm) boxplots

Fig. 2. Boxplots of Dice and Hausdorf distance values for pCT and dMRI ROIs. *A. Dice boxplots, B. Maximum HD (mm) boxplots, C. Average HD (mm) boxplots.*

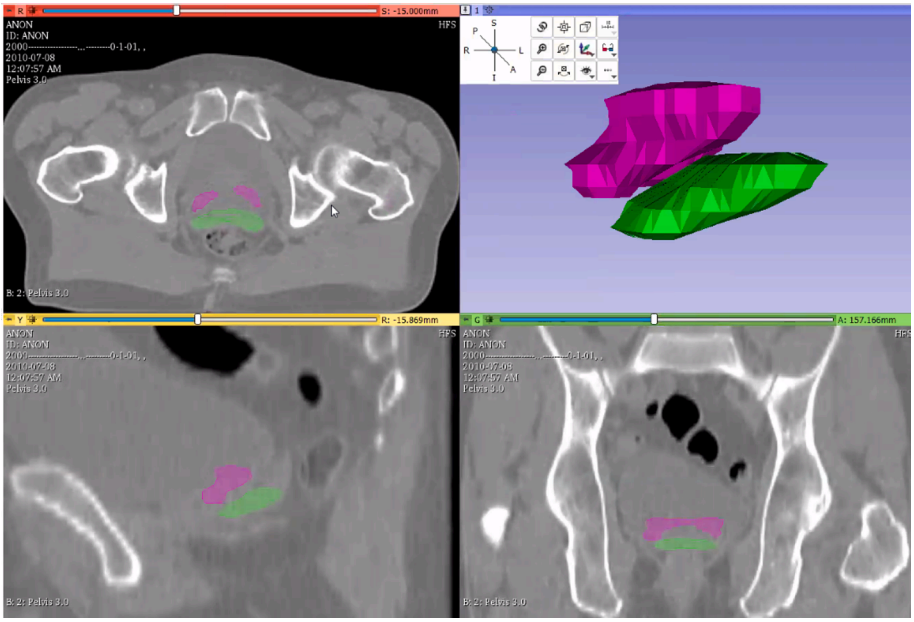

Fig. 3. Example of similar seminal vesical volume with minimal overlap. *3D Slicer Image of SV location in dMRI (pink) and pCT (green) scans on transverse, sagittal and coronal medical imaging planes, and 3D generated image. Abbreviations: SV = seminal vesicle, dMRI = diagnostic magnetic reasonance imaging, pCT = planning CT.* (For interpretation of the references to colour in this figure legend, the reader is referred to the web version of this article.)

best for the pCT scans.

As depicted in Table 3, some of the positive and negative predictive metrics generated values of NA. These correspond to when multiple zeros are reported in the confusion matrices for the predictions (Supporting Information) and therefore the ratios cannot be mathematically calculated.

Discussion

This study aimed to determine the feasibility of incorporating dMRI anatomical variables in Jones et al's [9,10] previously developed predictive models to assess individual patient HS benefit. In the evaluation of the similarity between dMRI and pCT ROIs, few had statistically significant differences. The model performance metrics indicated a trend that the pCT data performed slightly better than the dMRI overall, however, results interchanged depending on model type and the outcomes of interest. On average this ranged from a 0–0.25 difference in accuracy results to predict actual patient outcomes. The results indicate that further prospective studies and re-tuning of the model with dMRI anatomical information is worth investigation.

Only slight differences were observed between the dMRI and pCT ROI variables. The prostate Dice value of 0.81 comparing pCT to dMRI

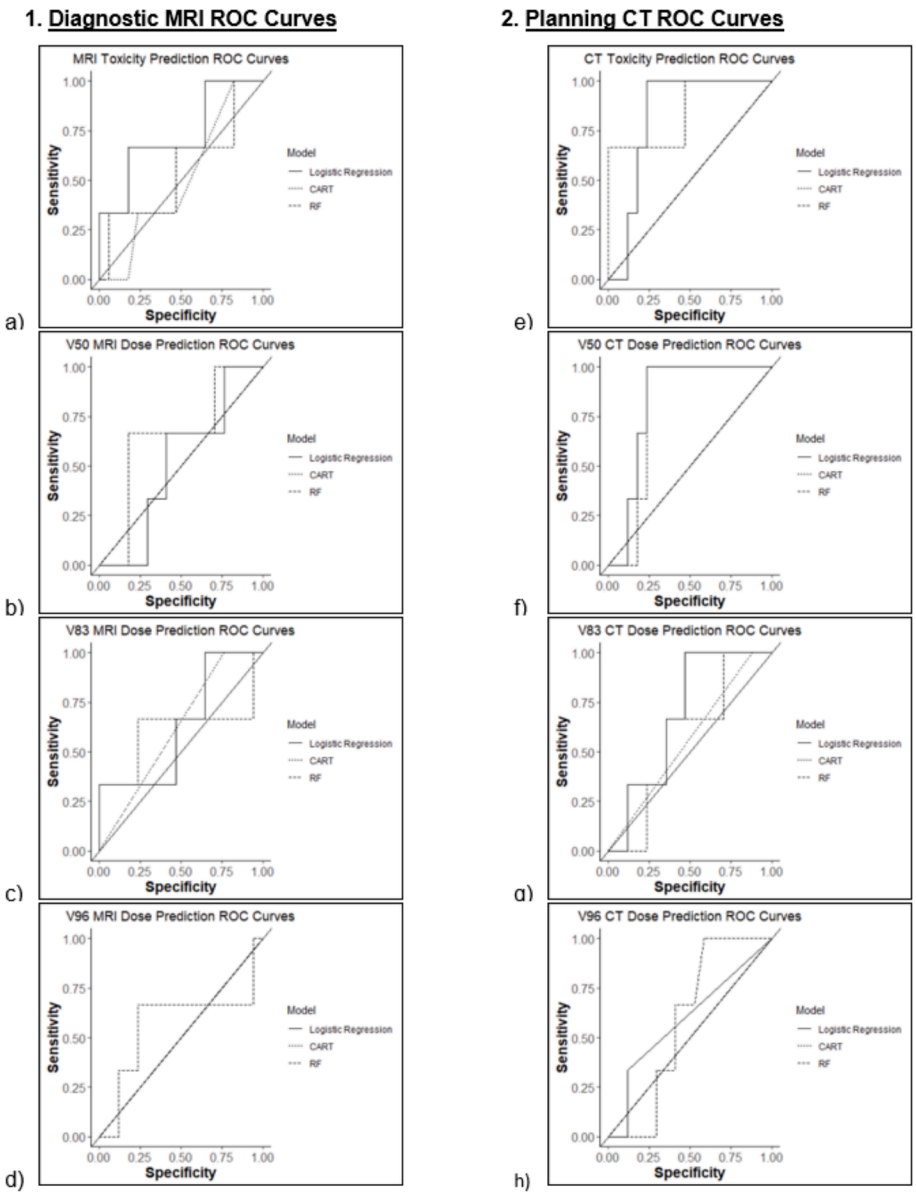

Fig. 4. ROC Plots for dMRI and pCT Toxicity and Dose Level Predictions. *a-d: dMRI ROC curves, e-f: pCT ROC curves. Abbreviations: ROC = receiver operator curves, dMRI = diagnostic magnetic reasonance imaging, pCT = planning CT.*

across all patients indicated a high degree of overlap, comparable to a Dice of 0.83 from an interobserver contouring study for male pelvic structures [21]. This was similar to the rectum ROI results which generated a Dice of 0.71. This is a clinically relevant result, however, is lower than the mentioned interobserver study's 0.93 value [21]. The lower Dice in this study may be attributed to variability in rectal filling between the dMRI and pCT rather than differences in multiple observers contouring the rectum on the same images. Conversely, a low degree of overlap was observed for the SV ROIs, with a Dice of 0.47. In the total 20 patients, two generated an SV Dice of 0. While it is reported in literature that smaller organs typically receive lower Dice scores [22] variable bladder and rectal filling between the dMRI and pCT images may have also contributed to the Dice for the SVs. The SV contours generated by radiation oncologists are influenced by extent or grade of disease. This was addressed by investigators contouring the same number of slices on the dMRI as pCT starting from the inferior aspect of the SVs. Although there were discrepancies between SV spatial location, only 0.23 cm^3 difference was perceived between the dMRI and pCT mean volumes of the organ across all patients.

As stated in the results, minimal differences in the prediction performance metrics of the models were observed between the dMRI and pCT images used. The average for the model performance metric of accuracy across all models indicated that there was a trend of pCT performing slightly better than dMRI. The same trend was also witnessed for the AUC performance metric with pCT resulting in higher clinical values (>0.7). However, the development of the models has a strong dependency on the data that is included in the training data set, and as the training dataset for the models was pCT data, it can explain the marginally lower accuracies and AUCs of dMRI predictions. General scrutiny of the results indicates the direction that the models produced (either Y or N to colonoscopy) was the same for both imaging modalities. Overall, the SML model that performed best for dMRI information was RF across all toxicity and dose predictions. This is comparable to the results of Jones et al's study [9]. This is a sub topic in need of more in-depth research to validate this outcome, however, whilst the same cohort of patients has been used for this study as the original research that developed the SML models and therefore this analysis cannot be classified as an external method of validation, it is an interesting finding

Table 3
Model performance metric outcomes for toxicity and dose level predictions across both dMRI and pCT scans.

	Toxicity Prediction			Dose Levels								
				V50			V83			V96		
Imaging Modality	Model Performance Metrics	Random Forest	Logistic Regression	CART	Random Forest	Logistic Regression	CART	Random Forest	Logistic Regression	CART	Random Forest	Logistic Regression	CART
Diagnostic MRI													
	Accuracy	0.85	0.85	0.80	0.60	0.50	0.85	0.30	0.15	0.35	0.15	0.85	0.15
	Sensitivity	0.94	1.00	0.94	0.65	0.53	1.00	0.24	0.00	0.24	0.06	1.00	0.00
	Specificity	0.33	0.00	0.00	0.33	0.33	0.00	0.67	1.00	1.00	0.67	0.00	1.00
	Lower CI	0.62	0.62	0.56	0.36	0.27	0.62	0.12	0.03	0.15	0.03	0.62	0.03
	Upper CI	0.97	0.97	0.94	0.81	0.73	0.97	0.54	0.38	0.59	0.38	0.97	0.38
	Pos Predictive	0.89	0.85	0.84	0.85	0.82	0.85	0.80	NA	1.00	0.50	0.85	NA
	Neg Predictive	0.50	NA	0.00	0.14	0.11	NA	0.13	0.15	0.19	0.11	NA	0.15
	AUC	0.55	0.73	0.50	0.65	0.51	0.50	0.61	0.63	0.62	0.57	0.50	0.50
Planning CT													
	Accuracy	0.95	0.85	0.75	0.75	0.75	0.85	0.45	0.30	0.25	0.20	0.85	0.15
	Sensitivity	1.00	1.00	0.82	0.76	0.71	1.00	0.41	0.18	0.12	0.06	1.00	0.00
	Specificity	0.67	0.00	0.33	0.67	1.00	0.00	0.67	1.00	1.00	1.00	0.00	1.00
	Lower CI	0.75	0.62	0.51	0.51	0.51	0.62	0.23	0.12	0.09	0.06	0.62	0.03
	Upper CI	0.10	0.97	0.91	0.91	0.91	0.97	0.68	0.54	0.49	0.44	0.97	0.38
	Pos Predictive	0.94	0.85	0.88	0.93	1.00	0.85	0.88	1.00	1.00	1.00	0.85	NA
	Neg Predictive	1.00	NA	0.25	0.33	0.38	NA	0.17	0.18	0.17	0.16	NA	0.15
	AUC	0.84	0.47	0.65	0.78	0.82	0.50	0.57	0.69	0.56	0.58	0.59	0.50

Abbreviations: MRI, CT, CI, V50, V83, V96, AU.

nonetheless that dMRI toxicity and dose predictions did not drastically differ to the pCT data. This outcome highlights the potential generalisability of Jones et al's [9] developed models and the possibility of achieving good predictive outcomes if re-tuning of the models were applied on the dMRI data [23]. Current trends in SML development have shown the value of re-tuning pre-trained models on new but smaller data sets to achieve good model performance in a process known as transfer learning [23]. This is an area worth exploring for this scenario, or for the external application of the models in a different department where the patient cohort distribution is likely to be varied.

Overall, the outcomes observed are encouraging, but not without the caveats of being a pilot study. The data underpinning the models were based on a small cohort of patients collected across several years of clinical practice, potentially introducing variations in inter-plan quality, clinical goals, and differences in PTV margins. In the current pilot study investigating the feasibility of using dMRI to generate the ROI variables 20 of the 176 patients whose data was used to develop the models was included. On a number of occasions NA values were calculated in the confusion matrices due to class imbalance. The class imbalance on a larger sample size can be managed using a synthetic minority oversampling technique (SMOTE) but is more challenging in small sample sizes. The variation in bladder and bowel preparation between the two image modalities was mitigated by using overlap ROIs that represented spatial relationships in Jones et al's study [9]. The bowel preparation differences likely contributed to the statistical significance between ROI overlap and Dice scores. The excellent soft tissue delineation in dMRI scans may have impacted prostate contours and subsequent performance in the statistical models. Additionally, the dMRI scan length did not often image the full length of rectum which is contoured in treatment planning and used for dosimetric volume histograms. Using dMRI scans that include all the pelvic anatomy is an important consideration in future studies. Alternatively, altering the variable ROIs to only include the rectum truncated at the superior and inferior ends of the prostate (or clinical target volume) could acquire more accurate data for use in dMRI modelling. This illustrates the importance of re-training the model with dMRI data. Ideally, the model should be retrained with dMRI data or re-tuned to the dMRI data if using a transfer learning approach and externally validated using data not included in re-training [24]. The results of this study are encouraging and indicate that it is worth retraining these models with dMRI anatomy for more accurate clinical implementation and with contemporary data to meet regulatory and governing body guidelines.

Conclusion

This study evaluated the feasibility of incorporating dMRI data in Jones et al's[9] SML models as a decision support tool for the selective use of HS in radiation therapy treatments for prostate cancer patients. The ROI comparison indicated insignificant variations in size and distance metrics between the dMRI and pCT scans. The dMRI prediction results indicated good discriminative ability for predicting class outcomes and all results were comparable to the CT outputs, albeit performing slightly worse overall. Further retraining of the current predictive models on dMRI anatomy and ensuring consistent scan protocols could assist in the routine implementation of this process in radiation therapy to facilitate HS clinical decisions.

Waiver of patient consent

This is a retrospective case study. Patient consent has been waived by Ethic committee.

Ethics

Institutional ethics was granted to conduct this study for the retrospective use of patient data (Princess Alexandra Hospital HREC ID: HREC/2020/QMS/68726, Queensland University of Technology ID: 2000001100).

Declaration of competing interest

The authors declare that they have no known competing financial interests or personal relationships that could have appeared to influence the work reported in this paper.

Appendix A. Supplementary data

Supplementary data to this article can be found online at https://doi.org/10.1016/j.tipsro.2025.100305.

References

[1] Payne HA, Jain S, Peedell C, et al. Delphi study to identify consensus on patient selection for hydrogel rectal spacer use during radiation therapy for prostate cancer in the UK. BMJ Open 2022;12(7):e060506. https://doi.org/10.1136/bmjopen-2021-060506.
[2] Lambin P, van Stiphout RG, Starmans MH, et al. Predicting outcomes in radiation oncology–multifactorial decision support systems. Nat Rev Clin Oncol 2013;10(1):27–40. https://doi.org/10.1038/nrclinonc.2012.196.
[3] Paetkau O, Gagne IM, Alexander A. SpaceOAR© hydrogel rectal dose reduction prediction model: a decision support tool. J Appl Clin Med Phys 2020;21(6):15–25. https://doi.org/10.1002/acm2.12860.
[4] Vanneste BG, Hoffmann AL, van Lin EN, Van De Voorde L, Pinkawa M, Lambin P. Who will benefit most from hydrogel rectum spacer implantation in prostate cancer radiotherapy? a model-based approach for patient selection. Radiother Oncol 2016;121(1):118–23. https://doi.org/10.1016/j.radonc.2016.08.026.
[5] Mariados N, Sylvester J, Shah D, et al. Hydrogel spacer prospective multicenter randomized controlled pivotal trial: dosimetric and clinical effects of perirectal spacer application in men undergoing prostate image guided intensity modulated radiation therapy. Int J Radiat Oncol Biol Phys 2015;92(5):971–7. https://doi.org/10.1016/j.ijrobp.2015.04.030.
[6] Mahal BA, O'Leary MP, Nguyen PL. Hydrogel spacing for radiotherapy of prostate cancer: a review of the literature. Urol Pract 2014;1(2):79–85. https://doi.org/10.1016/j.urpr.2014.03.004.
[7] van Wijk Y, Vanneste BGL, Jochems A, et al. Development of an isotoxic decision support system integrating genetic markers of toxicity for the implantation of a rectum spacer. Acta Oncol 2018;57(11):1499–505. https://doi.org/10.1080/0284186x.2018.1484156.
[8] Vanneste BGL, Buettner F, Pinkawa M, Lambin P, Hoffmann AL. Ano-rectal wall dose-surface maps localize the dosimetric benefit of hydrogel rectum spacers in prostate cancer radiotherapy. Clin Transl Radiat Oncol 2019;14:17–24. https://doi.org/10.1016/j.ctro.2018.10.006.
[9] Jones S, Hargrave C, Deegan T, Holt T, Mengersen K. Comparison of statistical machine learning models for rectal protocol compliance in prostate external beam radiation therapy. Med Phys 2020;47(4):1452–9. https://doi.org/10.1002/mp.14044.
[10] Jones S, White N, Holt T, Graves N. Cost-effectiveness analysis of hydrogel spacer for rectal toxicity reduction in prostate external beam radiotherapy. J Med Imaging Radiat Oncol 2021;65(7):931–9. https://doi.org/10.1111/1754-9485.13311.
[11] Caine H, Whalley D, Kneebone A, McCloud P, Eade T. Using individual patient anatomy to predict protocol compliance for prostate intensity-modulated radiotherapy. Med Dosim Spring 2016;41(1):70–4. https://doi.org/10.1016/j.meddos.2015.08.005.
[12] Fischer-Valuck BW, Chundury A, Gay H, Bosch W, Michalski J. Hydrogel spacer distribution within the perirectal space in patients undergoing radiotherapy for prostate cancer: Impact of spacer symmetry on rectal dose reduction and the clinical consequences of hydrogel infiltration into the rectal wall. Pract Radiat Oncol 2017;7(3):195–202. https://doi.org/10.1016/j.prro.2016.10.004.
[13] Grossman CE, Folkert MR, Lobaugh S, et al. Quality metric to assess adequacy of hydrogel rectal spacer placement for prostate radiation therapy and association of metric score with rectal toxicity outcomes. Adv Radiat Oncol 2023;8(4):101070. https://doi.org/10.1016/j.adro.2022.101070.
[14] Pathmanathan AU, McNair HA, Schmidt MA, et al. Comparison of prostate delineation on multimodality imaging for MR-guided radiotherapy. Br J Radiol 2019;92(1095):20180948. https://doi.org/10.1259/bjr.20180948.
[15] Cui S, Tseng HH, Pakela J, Ten Haken RK, El Naqa I. Introduction to machine and deep learning for medical physicists. Med Phys 2020;47(5):e127–47. https://doi.org/10.1002/mp.14140.
[16] Hargrave C, Deegan T, Poulsen M, Bednarz T, Harden F, Mengersen K. A feature alignment score for online cone-beam CT-based image-guided radiotherapy for prostate cancer. Med Phys 2018;45(7):2898–911. https://doi.org/10.1002/mp.12980.
[17] Vaassen F, Hazelaar C, Vaniqui A, et al. Evaluation of measures for assessing time-saving of automatic organ-at-risk segmentation in radiotherapy. Phys Imaging Radiat Oncol 2020;13:1–6. https://doi.org/10.1016/j.phro.2019.12.001.

[18] Fabri D, Zambrano V, Bhatia A, et al. A quantitative comparison of the performance of three deformable registration algorithms in radiotherapy. Z Med Phys 2013;23(4):279–90. https://doi.org/10.1016/j.zemedi.2013.07.006.
[19] US Department of Health and Human Services. Common Terminology Criteria for Adverse Events (CTCAE) Version 5. National Institutes of Health, National Cancer Institute. Updated November 27 2017. Accessed 14 January, 2025. https://ctep.cancer.gov/protocolDevelopment/electronic_applications/ctc.htm.
[20] Hosmer DW, Lemeshow S, Sturdivant RX, ProQuest. Applied logistic regression. 3rd / David W. Hosmer, Stanley Lemeshow, Rodney X. Sturdivant. ed. Wiley series in probability and statistics. Wiley; 2013.
[21] Roach D, Holloway LC, Jameson MG, et al. Multi-observer contouring of male pelvic anatomy: Highly variable agreement across conventional and emerging structures of interest. J Med Imaging Radiat Oncol 2019;63(2):264–71. https://doi.org/10.1111/1754-9485.12844.
[22] Yaver M, Foo A, Larsen T, et al. Consistency of organ geometries during prostate radiotherapy with two different bladder and bowel regimens. J Med Imaging Radiat Sci 2015;46(4):380–7. https://doi.org/10.1016/j.jmir.2015.09.001.
[23] Barragán-Montero A, Bibal A, Dastarac MH, et al. Towards a safe and efficient clinical implementation of machine learning in radiation oncology by exploring model interpretability, explainability and data-model dependency. Phys Med Biol 2022;67(11). https://doi.org/10.1088/1361-6560/ac678a.
[24] Steyerberg EW, Moons KG, van der Windt DA, et al. Prognosis research strategy (PROGRESS) 3: prognostic model research. PLoS Med 2013;10(2):e1001381. https://doi.org/10.1371/journal.pmed.1001381.